(2)

AD_____

MIPR NO: 92MM2515

TITLE: ARMY HIGH-PERFORMANCE COMPUTING RESEARCH CENTER FOR THE U.S. ARMY MEDICAL RESEARCH INSTITUTE OF INFECTIOUS DISEASES

PRINCIPAL INVESTIGATOR: Jagdish Chandra
Mark A. Olson

CONTRACTING ORGANIZATION: U.S. Army Research Office
P.O. Box 12211
Research Triangle Park
North Carolina 27709-2211

REPORT DATE: April 1, 1993

TYPE OF REPORT: Midterm Report

PREPARED FOR: U.S. Army Medical Research and Development Command, Fort Detrick
Frederick, Maryland 21702-5012

DISTRIBUTION STATEMENT: Approved for public release; distribution unlimited

The findings in this report are not to be construed as an official Department of the Army position unless so designated by other authorized documents.

REPORT DOCUMENTATION PAGE

Form Approved
OMB No. 0704-0188

1. AGENCY USE ONLY *(Leave blank)*	2. REPORT DATE	3. REPORT TYPE AND DATES COVERED
	1 April 1993	Midterm Report (9/28/92-3/31/93)

4. TITLE AND SUBTITLE
Army High-Performance Computing Research Center for the U.S. Army Medical Research Institute of Infectious Diseases

5. FUNDING NUMBERS
MIPR No.
92MM2615

6. AUTHOR(S)
Jagdish Chandra
Mark A. Olson

7. PERFORMING ORGANIZATION NAME(S) AND ADDRESS(ES)
U.S. Army Research Office
P.O. Box 12211
Research Triangle Park, North Carolina 27709-2211

8. PERFORMING ORGANIZATION REPORT NUMBER

9. SPONSORING / MONITORING AGENCY NAME(S) AND ADDRESS(ES)
U.S. Army Medical Research & Development Command
Fort Detrick,
Frederick, Maryland 21702-5012

10. SPONSORING / MONITORING AGENCY REPORT NUMBER

11. SUPPLEMENTARY NOTES

12a. DISTRIBUTION AVAILABILITY STATEMENT
Approved for public release; distribution unlimited

12b. DISTRIBUTION CODE

13. ABSTRACT *(Maximum 200 words)*

Computer simulation methods have been used to analyze the structural interactions and energetics governing the binding of substrates formycin 5′-monophosphate (FMP) and adenyl(3′→5′)guanosine (ApG) in the ricin A-chain active site. The studies undertaken showed the average simulation structures of the substrate-bound enzyme to be in good accord with the observed X-ray crystal structures in reproducing an overall binding mode. However, for FMP there are significant differences in the location and binding of the phosphate group. Free-energy simulation methods have been employed to explore several structural motifs of FMP which would have a greater binding affinity for the active site. It is shown that ricin A-chain has a preference for FMP over analogs 2-amino formycin 5′-phosphate and 2-hydroxyl formycin 5′-phosphate. Using the binding motif of the adenine ring from the average simulation structures, several substituents have been appended to the base with removal of the ribose and phosphate group leading to the design of new ligands for ricin. These potential antidotes are being further evaluated by molecular-dynamics simulations to determine the relative binding affinities.

14. SUBJECT TERMS	15. NUMBER OF PAGES
Ricin; Molecular modeling; structure-based ligand design; BD; RA IV	16. PRICE CODE

17. SECURITY CLASSIFICATION OF REPORT	18. SECURITY CLASSIFICATION OF THIS PAGE	19. SECURITY CLASSIFICATION OF ABSTRACT	20. LIMITATION OF ABSTRACT
Unclassified	Unclassified	Unclassified	Unlimited

FOREWORD

Opinions, interpretations, conclusions and recommendations are those of the author and are not necessarily endorsed by the US Army.

____ Where copyrighted material is quoted, permission has been obtained to use such material.

____ Where material from documents designated for limited distribution is quoted, permission has been obtained to use the material.

____ Citations of commercial organizations and trade names in this report do not constitute an official Department of Army endorsement or approval of the products or services of these organizations.

____ In conducting research using animals, the investigator(s) adhered to the "Guide for the Care and Use of Laboratory Animals," prepared by the Committee on Care and Use of Laboratory Animals of the Institute of Laboratory Resources, National Research Council (NIH Publication No. 86-23, Revised 1985).

____ For the protection of human subjects, the investigator(s) adhered to policies of applicable Federal Law 45 CFR 46.

____ In conducting research utilizing recombinant DNA technology, the investigator(s) adhered to current guidelines promulgated by the National Institutes of Health.

____ In the conduct of research utilizing recombinant DNA, the investigator(s) adhered to the NIH Guidelines for Research Involving Recombinant DNA Molecules.

____ In the conduct of research involving hazardous organisms, the investigator(s) adhered to the CDC-NIH Guide for Biosafety in Microbiological and Biomedical Laboratories.

Mark A. Olson 3/29/93

PI - Signature Date

TABLE OF CONTENTS

INTRODUCTION

In nature, evolution has created proteins which are toxic to cells. Well-studied classes of such cytotoxic proteins are the plant and bacterial toxins. Among the plant toxins, the protein ricin is exceptionally toxic; a single molecule is sufficient to kill a cell [1,2]. Isolated from the seeds of *Ricinus communis*, ricin is a heterodimeric protein consisting of a 267-residue cytotoxic A-chain (RTA) linked by a disulfide bond to a B-chain (RTB) of 262 residues, which binds to galactose residues present on various cell surface glycoproteins and glycolipids. The A-chain functions by inhibiting the synthesis of protein in eukaryotic cells through the hydrolysis of an *N*-glycosidic bond of the adenosine residue in 28S ribosomal RNA [3,4]. This reaction is remarkably specific in that deadenylation occurs at a single nucleotide from amongst the 7000 in the organelle. It has been shown that RTA will also catalyze a synthetic GAGA tetraloop oligoribonucleotide with three base-pairs [5]. The nature of the base-pairs does not influence recognition or catalysis by RTA, whereas the position of the tetranucleotide in the loop sequence is critical.

The X-ray structure of ricin at a refinement of 2.5 Å has been reported by Robertus and coworkers [6,7]. Eight invariant residues appear to be involved in creating or stabilizing the putative active site. In addition, there are five highly conserved polar residues located in the active-site cleft. From mutagenic studies, Glu 177 and Arg 180 appear to be key catalytic residues [8,9]. The conversion of Glu 177 to the corresponding amide decreases activity 180-fold [8] and the conversion of Arg 180 to histidine results in a 1000-fold reduction in activity [9]. A mechanism of action has been proposed which involves binding of the substrate adenosine in a *syn*

configuration with an oxycarbonium ion stabilization on the ribose by Glu 177 and anion stabilization through protonation at N-3 by Arg 180 [8,10].

Recently, X-ray crystallography has resolved the three-dimensional structure of formycin 5'-monophosphate (FMP) and adenyl(3'→5')guanosine (ApG) bound in the active site of RTA [10]. These two nucleotide compounds are thought to mimic certain elements of the rRNA substrate, in particular the binding of the adenine ring. Both structures show the adenine ring in a *syn* conformation stacked between a pair of tyrosines. In addition, there are several specific hydrogen bonds with polar groups of the binding pocket which are thought to discriminate between adenine and guanine.

While the structural binding motif of the adenine ring has emerge from these studies, the dynamics and energetics of native versus substrate-bound RTA remains largely unknown. Because of the difficulties encountered in experimental approaches to the problem, theoretical studies of the interaction of the RTA molecule with nucleotides may be of great assistance in the interpretation of biophysical data and the development of selective inhibitors to ricin intoxication.

This report presents molecular-dynamics (MD) simulation studies of the binding of substrates with ricin A-chain. In the present work, the MD simulation method has been applied to the binding of substrates FMP (structure I), ApG (structure II), and is currently being applied to the hexanucleotide CGAGAG. In addition to the biomolecular dynamics of the RTA-FMP complex, relative changes in binding free energies have been estimated for FMP analogs using a thermodynamic integration technique [11] applied to amino substitutions at the 2 and 2' positions and hydroxyl substitution at the 2' position.

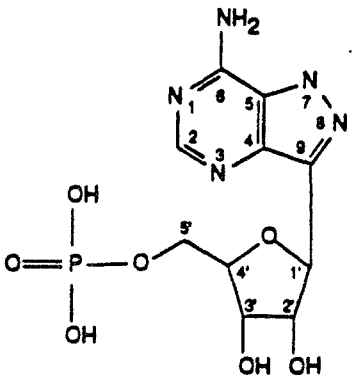

I

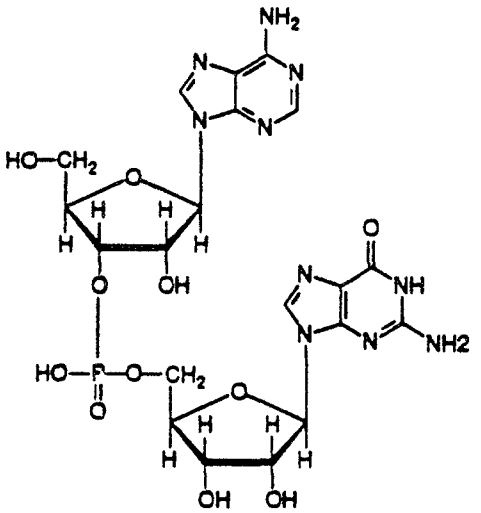

II

Molecular-dynamics simulations of the mono and dinucleotides were carried out initiated from the X-ray crystal structures of the FMP- and ApG-bound enzyme refined to 2.8 Å and 3.0 Å, respectively. For the CGAGAG substrate-RTA study, simulations are in progress employing a hypothetical model constructed by Monzingo and Robertus [10] immersed in solvent water.

Complementary with the molecular simulation efforts, *de novo* design studies of A-chain inhibitors are being carried out utilizing a rule-based search algorithm [12] aimed at determining small molecules and fragments which may fit the nonbonded contact geometry of the active site. This effort combined with molecular simulations should yield a computational framework for exploring the rational design of ligands which may function as transition-state inhibitors to ricin.

METHODS, RESULTS AND DISCUSSION

In this section we present the computational methods employed and the results obtained for the molecular modeling studies outlined above. Discussion of these relative to the goals of the research is presented.

Molecular Modeling Methodology

Molecular-dynamics simulations were performed for the native and substrate-bound RTA using the program DISCOVER [13] with force fields modeled using either AMBER [14] or CVFF [15]. Two sets of simulations were carried out for the FMP-bound enzyme: (1) AMBER was used with substrate charges determined by electrostatic potential fitting [16] to a single-point wave function with an 6-31G* basis set using Gaussian 92 [17]; (2) CVFF was used with charges derived from the nucleic acid library calibrated via MNDO [18] calculations with an STO-3G basis set. Parameters for the enzyme were taken from the AMBER or CVFF amino acid residue library. Simulations of the FMP analogs together with ApG- and CGAGAG-bound enzymes were carried out employing CVFF and AMBER, respectively, with charges calculated as described above.

The native enzyme and substrate-bound RTA structures were simulated by constructing an active-site region composed of part of the protein and ligand inside a 12-Å spherical boundary as derived from the various crystal structures (see Figures 1a-c). Amino acid residues lying in the outer shell were fixed at their initial positions and should not introduce significant phase-space sampling errors. Active-site regions for the complexed and free structures were immersed in a 8-Å deformable layer of water. Water was represented using a flexible SPC potential [19]. Simulations of the various RTA-substrate active regions consisted of: (1) FMP or analog plus 63 RTA residues (1026 protein atoms), two sodium counterions, and 362 water molecules; (2) ApG plus 83 residues (1396 atoms), one counterion, and 544 water molecules; and (3) CGAGAG plus 144 residues (2350 atoms), six counterions, and 1231 solvent molecules. For the free enzyme system, simulations were carried out for the same active region as in the CGAGA-bound RTA simulation plus 1210 water molecules.

Simulations were initiated with 2000 cycles of minimization using a steepest descent algorithm followed by 30-ps equilibration. The initial atomic velocities were assigned from a Gaussian distribution corresponding to a temperature of 300 K. Nonbond interactions were smoothed to zero beyond 9.0 Å and a constant dielectric ($\varepsilon = 1$) was used. All hydrogens were treated explicitly employing a 1.0 fs timestep for integrating the equations of motion. Ensemble averages were determined from a production runs of 100-300 ps with coordinates, velocities, and energies saved every 50 timesteps (0.05 ps) for further analysis. All simulations were carried out on a CRAY Y-MP located at the National Cancer Institute, Frederick Cancer Research and Development Center.

(Fig. 1a)

(Fig. 1b)

(Fig. 1c)

Figure 1. Stereoviews of substrate-bound ricin A-chain. (a) RTA-FMP; (b) RTA-ApG; and (c) RTA-CGAGAG.

For estimating the relative binding affinity of FMP and its analogs (denoted as FMP′) with the active site of RTA, we make use of the following thermodynamic cycle: $\Delta(\Delta A) = \Delta A_{inhib'} - \Delta A_{inhib} = \Delta A_{bind} - \Delta A_{solv}$, where ΔA_{inhib} and $\Delta A_{inhib'}$ are the Helmholtz free energy of binding for substrates FMP and FMP′, respectively; ΔA_{solv} represents the solvation free-energy difference between FMP and FMP′, and ΔA_{bind} represents the binding free-energy difference between FMP and FMP′ in the RTA

active site. Molecular-dynamics simulations were performed for a series of small discrete transformations of FMP into the 2- and 2′-amino and 2-hydroxyl analogs. The force fields were modeled using the CVFF. Simulations of the substrate-bound enzyme employed the active-region methodology as described above. For the unbound ligand systems, simulations were carried out by placing the solute from the X-ray crystal structure in a cubic box of length 27 Å containing 632 water molecules plus counterions. Periodic boundary conditions were utilized in these latter set of calculations in reducing edge effects.

Free-energy simulation protocol consisted of all systems simulated at ten values of the advancement coordinate λ connecting the initial (crystal structure) state to the mutated state. The λ_1 simulations were initiated with 400 cycles of minimization using a steepest descent algorithm plus 1000 cycles of minimization via a conjugate gradient algorithm followed by 10-ps equilibration. Simulations for λ_2, λ_3, ..., λ_9 were carried out following a 5-ps equilibration started from the final step of the previous simulation. The λ_{10} simulations were initiated with a 10-ps equilibration.

Recent advances on new methods for the *de novo* design of enzyme inhibitors have lead to the development of a computer program called LUDI [12]. As described in the literature, LUDI can append new substituents onto an already existing ligand (*e.g.*, FMP) in such a way that hydrogen bonds are formed with the protein and hydrophobic pockets are filled with suitable sidechains of the ligand.

For ricin A-chain, efforts are currently in progress applying LUDI to the design of

ligands which may function as antidotes. This effort offers the important possibility to design new substituents for the adenine ring given the fact that RTA recognizes both FMP and ApG.

Results and discussion

Examination of the averaged intramolecular and nonbonded interaction energies computed over 100 ps for the RTA-FMP simulation model where FMP was modeled as a dianion shows significant deviation in the binding electrostatic interactions between the substrate and enzyme as compared with the corresponding values for the X-ray structure. Superposition of the average simulation structure and the crystal structure is shown in Figure 2. In general, the simulation structure agrees with the observed structure by Monzingo and Robertus [10], with several important differences as described below. In accord with the crystal structure, the simulation structure shows the formycin ring conformationally stacked between the rings of tyrosines 80 and 123. These two residues make strong packing interactions with the substrate stabilizing the binding complex. The hydroxyl group of Tyr 80 further stabilizes the binding of FMP by making several distant electrostatic interactions with the pyrazolopyrimidine moiety and the ribose.

The simulation structure and the crystal structure show FMP strongly interacting with polar groups of the active-site cavity. Most important are several backbone carbonyls that point toward the center of positive charge density of the formycin ring and make hydrogen bonds to its protons. Both structures show N-6 donating a hydrogen bond to the carbonyls of Val 81 and Gly 121, and a hydrogen bond between N-7 and the carbonyl of Gly 121. In addition, N-1 is shown to accept a hydrogen bond

from the backbone amide group of Val 81.

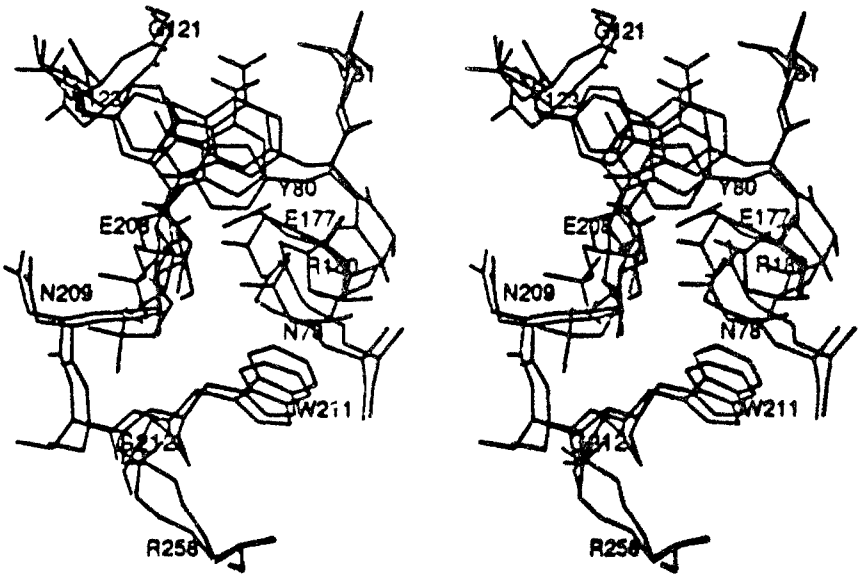

Figure 2. Stereoview showing a superposition of the average dianion model simulation structure and X-ray crystal structure for the binding RTA-FMP complex.

A key feature of the binding of FMP is the electrostatic interactions with charged residues of the active site, principally Glu 177, Arg 180, and Glu 208. The guanidinium group of Arg 180 donates a strong hydrogen bond to N-3 of the formycin ring. From the simulation structure the carboxylate of Glu 177 and the backbone carbonyl of Glu 208 make strong electrostatic interactions with the ribose O-2′ and O-3′, respectively. From the X-ray structure the ribose O-2′ appears to be weakly hydrogen bonded to both glutamates.

The substrate FMP makes important binding interactions with the side chain of Ile 172 and amide groups of Asn 122, Trp 211, and Gly 212. Ile 172 packs against the

formycin ring and makes a favorable contribution through van der Waals interactions. The amide backbone of residues 122, 211, 212 exert their effect on the binding of FMP primarily through long-range electrostatic interactions with N-7 for residue 122, and both the ribose O-3′ and phosphate group for residues 211 and 212.

Structural differences between the X-ray crystal structure and the average simulation structure for the dianion model system are derived primarily from interactions between the phosphate group and protein atoms. From the X-ray structure the phosphate group projects out of the binding pocket into the solvent and makes a long-range (4.7 Å) electrostatic interaction with the positively charged guanidinium group of Arg 258. The average simulation structure shows the phosphate group at a lower position as a result of strong ion-pair interactions with Arg 258 and long-range interactions with Arg 180. Nonbonded interaction energy for residue 258 corresponding to the simulation structure is approximately two-fold greater than the crystal structure.

The average simulation structure shows the phosphate group strongly interacting with eight water molecules, three of which are bridge forming waters with side chains of Tyr 80, Gly 212, and Arg 258. Because of strong electrostatic interactions of the phosphate group with protein atoms, the simulation structure suggests a less restrictive solvent accessible surface area for the ribose than observed in crystal structure showing two possible hydrogen bonds with water molecules, one bridging Gly 212 and the phosphate group. The simulation also clearly shows the desolvation of several key active-site residues upon binding of FMP. A comparison of the RTA-FMP simulation structure with the average MD simulation structure of the

native enzyme shows the loss of approximately five water molecules bound to residues Glu 177, Arg 180, and Glu 208. These waters are thought to be critical nucleophiles in the development of a transition-state like binding complex of the ribosome [8,10].

Examination of the structures of FMP in the RTA active site during the 100-ps molecular-dynamics simulation shows noticeable thermal fluctuations in the phosphate backbone and formycin ring while the sugar remained relatively rigid along the ribose O-4′ backbone and somewhat flexible in the hydroxyl groups. A comparison of the torsion angles describing the conformation of FMP obtained from the X-ray structure and the average simulation structure shows deviations in the calculated backbone torsion angles β and γ from the crystal structure of about 103° and 23°, respectively, and can be attributed to the significant interactions between protein atoms and the phosphate group of the simulation model. The simulation structure shows exocyclic and endocyclic torsions corresponding to a 2′-*endo* pucker in contrast to the 3′-*endo* configuration observed in the crystal structure. Calculated endocyclic torsions appear to be driven by interactions of the ribose ring with glutamates 177 and 208. From the crystal structure the formycin ring shows a high *syn* configuration with a torsion χ of about 128°, whereas the simulation model shows χ having a value near 80° ± 19°.

A set molecular-dynamics simulations were carried out for monoanionic and zwitterionic FMP structures employing the CVFF force fields. Like the dianion

simulation model results, the monoanion model shows significant variance in the computed electrostatic interaction energy with the crystal structure. Superposition of the average simulation structure and the X-ray crystal structure is shown in Figure 3. The simulation structure is found to be similar to that of the dianionic structure. Most noticeable difference, as expected, is in the interactions of the phosphate group with surrounding protein atoms. Interaction of FMP with the guanidinium group of 258 is reduced on average 25 kcal/mol from the dianion model. Accompanying this reduction is a favorable increase in long-range electrostatic interactions between the phosphate group and Arg 213 made possible in part by the reduction in the number of water molecules (from eight to four) solvating the phosphate moiety. Residues 177 and 208 appear to form strong hydrogen bonds with the hydroxyl groups of the sugar in agreement with the dianion model. For Arg 180, there appears to be a reduction in the magnitude of the electrostatic interactions with the ribose and phosphate group.

The FMP monoanion model calculated backbone torsion angles β and γ appear to deviate from the crystal structure by about 23° and 16°, respectively. The endocyclic torsions show somewhat better agreement with the crystal structure values than the dianion model results showing a 3′-*endo* configuration and the formycin ring appears to be in a high *syn* configuration with a torsion χ of about 130°.

Simulation results for the zwitterion model show significant deviation from the X-ray crystal structure in the interactions and conformations of FMP and several active-site residues (see Figure 3). Protonation of N-3 produces an approximate 3-Å shift and 40° rotation of the formycin ring from the average simulation monoanionic

structure. The van der Waals interaction energy contributions of residues 80 and 123 toward stabilizing the binding complex are substantially reduced from the crystal structure and anion simulations. Likewise, total nonbonded interactions between N-6 and the backbone carbonyl of Val 81 are reduced significantly.

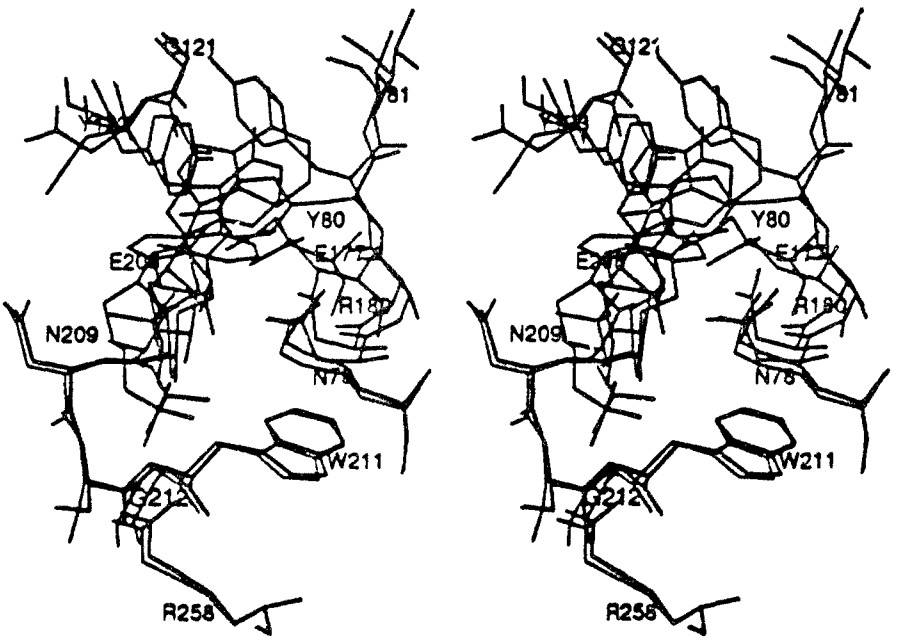

Figure 3. Stereoview showing a superposition of the average monoanion and zwitterion model simulation structures and X-ray crystal structure for the binding RTA-MP complex.

The average simulation structure of the zwitterion model shows Gly 121 making a hydrogen bond with N-6 rather than N-7 as in the anion model results, and several strong long-range electrostatic interactions between the formycin ring and aspartates 75, 96, and 100. Interactions with these latter residues, made possible by the

rotational shift in the formycin ring, contributes substantially towards stabilizing the binding complex and reflects a different binding mode of the formycin ring with the active site.

The calculated angles β and γ for the zwitterion model show deviations from the crystal structure of roughly 51° and 7°, respectively. Significant deviations are observed for the ribose endocyclic torsions, while the formycin ring shows a *syn* configuration with a torsion χ of about 141° in approximate agreement with the crystal structure.

A comparison of the three average simulation structures shows the magnitude of ligand binding interactions with the enzyme increases as zwitterionic > dianionic > monoanionic. As was discussed above, all three models predict significantly greater interaction energies than the crystal structure. Furthermore, each of the models predicts an average ligand conformation that differs from each other and the crystal structure, both qualitatively and quantitatively. From examination of the ligand position in the enzyme binding pocket and the type of structural interactions, the dianion and monoanion simulation models appear to be superior to the zwitterion model in reproducing the enzyme-ligand complex. The zwitterion model based on the phosphate group carrying a negative charge and the protonation of N-3 of the formycin ring predicts a ligand structure and binding mode inconsistent with the observed RTA-FMP crystal structure.

Several structural motifs constructed from the original FMP structure were investigated using free-energy simulation methods for the anion models. For the 2-

amino formycin 5′-phosphate analog transformation, the free energies calculated for the enzyme-bound ligand (ΔA_{bind}) predict the analog to interact more favorably with the enzyme in both dianion and monoanion simulation models. However, the *relative* binding free energies ($\Delta\Delta A$) predict the 2-amino analog to bind less strongly to RTA than does FMP itself. Selectivity reflects solvation effects, as it is less difficult to desolvate FMP than its 2-amino derivative. The lack of significant sensitivity in the relative free-energy change on the ionization state of the phosphate group suggests a dominate van der Waals component contribution to $\Delta\Delta A$.

Of the free-energy simulations for the 2-hydroxyl formycin 5′-phosphate analog, the monoanion model shows a greater relative binding affinity ($\Delta\Delta A$ =-1.8 kcal/mol) for the active site of RTA than the original FMP substrate. Analysis of the average end-point structure shows several changes in the structural interactions between the ligand and residues Tyr 80, Glu 177, and Arg 180. Most important, the carboxylate of 177 interacts favorably with the hydroxyl group. The formycin ring of the hydroxyl analog appears to be a high *syn* conformation (χ= 150°) and makes several strong interactions found in the FMP simulation structure, most notably interactions with the polar backbone of Val 81 and Gly 121 as well as packing interactions with Tyr 80 and Tyr 123. Finally, decomposition of $\Delta\Delta A$ shows a large electrostatic free-energy interaction component dominating the improved binding of the ligand.

As for the 2′-amino formycin 5′-phosphate analog, neither of the two simulation

models predict a relative increase in binding affinity for the enzyme. Both ΔA_{bind} and ΔA_{solv} show a decrease in favorable interactions with the enzyme and solvent, respectively.

Given the simulation results for the FMP dianion model (CVFF force fields with charges computed employing the nucleic acid library), a 200-ps molecular dynamics simulation of FMP was carried out with the AMBER force field with charges calculated at the *ab initio* level of 6-31G*. As in the preliminary studies of the RTA-FMP complex described above, the energy contribution that shows significant deviation is the electrostatic binding term. Analysis of the time development of the energy components in the simulation shows that the various energies are stable throughout the entire simulation of 200 ps and reveals that FMP is energetically near equilibrium.

Root-mean-square (RMS) deviation for the enzyme-substrate complex is roughly 0.6 Å and a fit of the substrate structures yields 0.8 Å. The simulation structure shows the substrate position shifted by approximately 1 to 3 Å with the largest Cartesian coordinate differences occurring in the phosphate group. This translation promotes favorable electrostatic interactions between the residues Asp 124 and Glu 127 and the ribose. In addition, the simulation structure shows strong electrostatic interactions between Arg 134 and the formycin ring. These interactions constitute one of two major differences with the simulations employing the CVFF force fields. The other difference deals with the torsion angles. From the simulation structure, the endocyclic and exocyclic torsions plus the glycosidic torsion are in good agreement with crystal structure. The backbone torsion β shows a variance of approximately 94°

from the crystal structure and like the CVFF calculations can be attributed to significant protein-phosphate interactions.

Molecular-dynamics simulations of the structural interactions governing the binding of ApG with the active of RTA were carried out for 300 ps. Figure 4 shows a superposition of the average simulation structure and X-ray crystal structure. The root-mean-square (RMS) deviation for the enzyme-substrate complex is roughly 0.69 Å and a fit of the substrate structures yields 1.5 Å. From the crystal structure, the adenine ring is conformationally stacked between the rings of tyrosines 80 and 123. Both residues provide efficient packing interactions stabilizing adenine binding. In addition, both tyrosines stabilize the binding of the guanosine ribose by making several long-range electrostatic interactions and van der Waals contacts. The simulation structure shows the substrate conformation shifted on average by 2 Å resulting in weaker van der Waals interactions for residues 80 and 123. A comparison of rotameric states for both tyrosines in the crystal structure and simulation structure shows for Tyr 80 χ_1 = (-153°, X-ray; -175°, simulation) and χ_2 = (-82°, X-ray; -104, simulation); for Tyr 123 χ_1 = (-81°, X-ray; -156°, simulation) and χ_2 = (-59°, X-ray; -64°, simulation).

From the X-ray structure, the binding of adenine involves the "solvation" of N-1 and the proton at N-6 by the backbone amide group and carbonyl of Val 81, respectively, and N-3 by the guanidinium group of Arg 180. There are no strong enzyme ion-pair interactions with imidazole ring. The nearest donor for N-7 is the amide backbone of Tyr 123 at distance of about 4 Å. In contrast, the average simulation structure shows a hydrogen bond between N-7 and Tyr 123 plus ion-pair

interactions between N-6 and the carbonyl of Gly 121 as well as interactions between N-3 and Arg 180. From the simulation structure the distance between N-1 and the amide group of Val 81 is roughly 4 Å versus 2 Å in the crystal structure. The combined effect of residues 81 and 121 is to stabilize the binding of ApG by -4.2 kcal/mol in the crystal structure and -2.3 kcal/mol in the simulation structure.

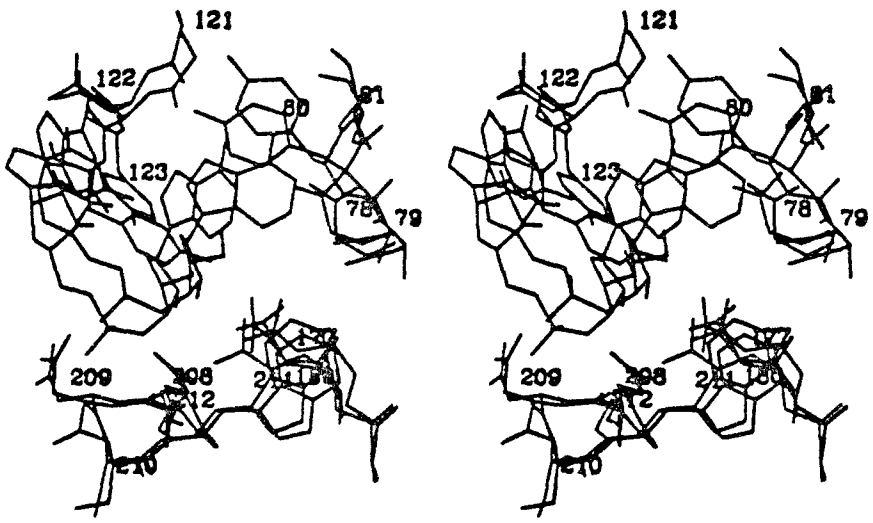

Figure 4. Stereoview showing a superposition of the average simulation structure and X-ray crystal structure for the binding RTA-ApG complex.

Both the crystal structure and simulation structure show the positively charged guanidinium group of Arg 180 making favorable binding interactions with adenosine ribose O-2′. Further long-range electrostatic interactions are made with the guanosine phosphate group stabilizing the binding of ApG.

Building on the average simulation structures for substrates FMP and ApG

bound in the RTA active site, design studies are being carried out aimed at determining new ligands with improved binding. Current efforts are directed at appending new substituents onto the existing FMP and ApG structures. Shown below (structure III) and in Figure 5 is an example of a proposed ligand structure constructed from molecular-dynamics simulations of the adenine-like ring in FMP bound to the active site of RTA.

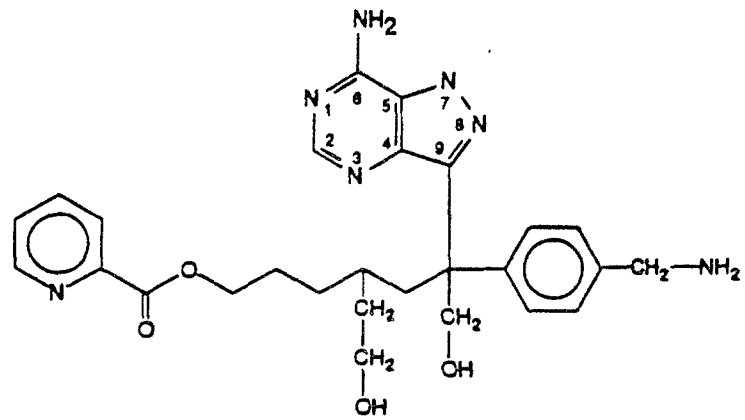

III

Energy refinement of the enzyme-ligand (structure III) complex has been carried out via energy minimization. Poor van der Waals contacts with the protein and poor internal geometries from linking multiple fragments have been removed. A rough measure of the fit and binding of a ligand is its total nonbonded interaction energy with the receptor. Calculations show that ligand III binds as strongly to ricin A-chain as the original substrate FMP determined by crystallography, but less than the molecular-dynamics simulation prediction. Nonetheless, this result is promising in that the

proposed ligand does not contain a highly charged phosphate group as compared with FMP, while having approximately the same interaction energy with the protein. More subtle energetic questions such as relative binding free energies necessary for accurate ligand design requires molecular-dynamics simulations.

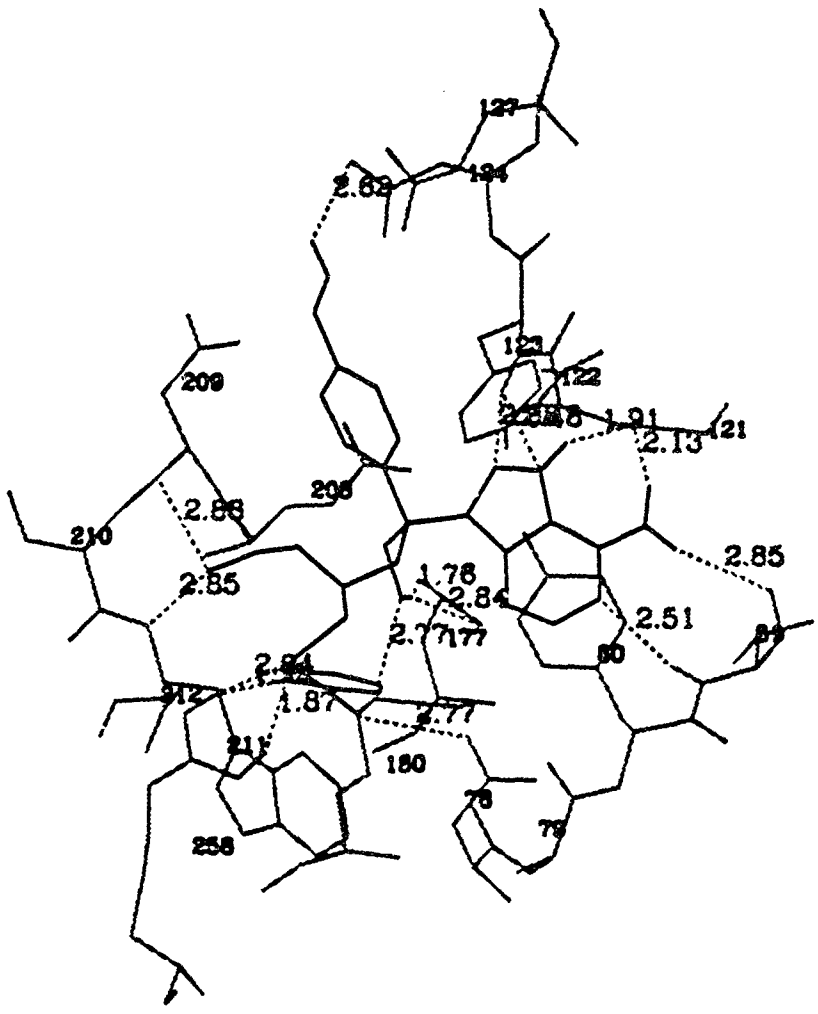

Figure 5. *De Novo* ligand design. Structure III in the active site of ricin A-chain.

CONCLUSIONS

Computer simulation methods have been used to analyze the structural interactions and energetics governing the binding of substrates formycin 5′-monophosphate and adenyl(3′→5′)guanosine in the ricin A-chain active site. The studies undertaken showed the average simulation structures of the substrate-bound enzyme to be in good accord with the observed X-ray crystal structures in reproducing an overall binding mode. However, for FMP there are significant differences in the location and binding of the phosphate group. Free-energy simulation methods have been employed to explore several structural motifs of FMP which would have a greater binding affinity for the active site. It is shown that ricin A-chain has a preference for FMP over analogs 2- and 2′-amino formycin 5′-phosphate and 2-hydroxyl formycin 5′-phosphate. Using the binding motif of the adenine ring from the average simulation structures, several substituents have been appended to the base with the removal of the ribose and phosphate group leading to the design of new ligands for ricin. These potential antidotes are being further evaluated by molecular-dynamics simulations to determine the relative binding affinities.

REFERENCES

[1] Eiklid, K., Olsnes, S & Pihl, A. (1980) *Expt. Cell Res.* **126**, 321.

[2] Olsnes, S. & Pihl, A. (1982) In *Molecular Action of Toxins and Virsuses* (Cohen, P. & van Heyningen, S., eds), pp.51-105, Elsevier Biomedical Press, New York.

[3] Endo, Y. & Tsurugi, K. (1987) *J. Biol. Chem.* **262**, 8128.

[4] Endo, Y., Mitsui, K., Motizuki, M. & Tsurugi, K. (1987) *J. Biol. Chem.* **262**, 5908.

[5] Glück, A., Endo, Y., & Wool, I.G. (1992) *J. Mol. Biol.*, **226**, 411.

[6] Katzin, B.J., Collins, E.J., & Robertus, J.D. (1991) *Proteins* ,**10**, 251.

[7] Rutenber, E., Katzin, B.J., Collins, E.J., Misna, D., Ernst, S.E., Ready, M.P., & Robertus, J.D. (1991) *Proteins,* **10**, 240.

[8] Ready, M. P., Kim, Y., & Robertus, J.D. (1991) *Proteins,* **10**, 270.

[9] Frankel, A., Welsh, P., Richardson, J., & Robertus, J.D. (1990) *Mol. Cell. Biol.*, **10**, 6257.

[10] Monzingo, A.F. & Robertus, J.D. (1992) *J. Mol. Biol.*, **227**, 1136.

[11] van Gunsteren, W.F. & Weiner, P.K. (ed.) *Computer Simulation of Biomolecular Ststems.* ESCOM. Leiden, (1989).

[12] Böhm, J.H. (1992) *J. Comput. -Aided Mol. Design*, 6, 69.

[13] Biosym Technologies, Inc., San Diego, CA.

[14] Weiner, S.J., Kollman, P.A., Nguyen, D.T., & Case, D.A. (1986) *J. Comp. Chem.*, **7**, 230-252.

[15] Dauber-Osguthorpe, P., Roberts, V.A., Osguthorpe, D.J., Wolff, J, Genest, M., & Hagler, A.T. (1988) *Proteins* , **4**, 31.

[16] Besler, B.H., Merz, K.M., Jr., & Kollman, P.A. (1990) *J. Comp. Chem.*, **11**, 431.

[17] Gaussian, Inc., Pittsburgh, PA.

[18] Stewart, J.J.P., MOPAC 5.0, QCPE, (1989) *QCPE Bull.*, **9**, 123.

[19] Teleman, O., Jönsson, B., & Engström, S. (1987) *Mol. Phys.*, **60**, 193.